Biophysical Journal Volume 68 June 1995 2404–2418

Parallel Inhibition of Active Force and Relaxed Fiber Stiffness by Caldesmon Fragments at Physiological Ionic Strength and Temperature Conditions: Additional Evidence That Weak Cross-Bridge Binding to Actin Is an Essential Intermediate for Force Generation

T. Kraft,* J. M. Chalovich,‡ L. C. Yu,§ and B. Brenner*

*Department of General Physiology, University of Ulm, Ulm, Germany; ‡Department of Biochemistry, East Carolina University Medical School, Greenville, North Carolina, USA; and §National Institutes of Health, Bethesda, Maryland, USA

ABSTRACT Previously we showed that stiffness of relaxed fibers and active force generated in single skinned fibers of rabbit psoas muscle are inhibited in parallel by actin-binding fragments of caldesmon, an actin-associated protein of smooth muscle, under conditions in which a large fraction of cross-bridges is weakly attached to actin (ionic strength of 50 mM and temperature of 5°C). These results suggested that weak cross-bridge attachment to actin is essential for force generation. The present study provides evidence that this is also true for physiological ionic strength (170 mM) at temperatures up to 30°C, suggesting that weak cross-bridge binding to actin is generally required for force generation. In addition, we show that the inhibition of active force is not a result of changes in cross-bridge cycling kinetics but apparently results from selective inhibition of weak cross-bridge binding to actin. Together with our previous biochemical, mechanical, and structural studies, these findings support the proposal that weak cross-bridge attachment to actin is an essential intermediate on the path to force generation and are consistent with the concept that isometric force mainly results from an increase in strain of the attached cross-bridge as a result of a structural change associated with the transition from a weakly bound to a strongly bound actomyosin complex. This mechanism is different from the processes responsible for quick tension recovery that were proposed by Huxley and Simmons (Proposed mechanism of force generation in striated muscle. *Nature.* 233:533–538.) to represent the elementary mechanism of force generation.

INTRODUCTION

In generating active force, cross-bridges in striated muscle pass through several different states. These states are of two main types: the non-force-generating, or weakly binding, cross-bridge states and the force-generating, or strongly binding, cross-bridge states (Lymn and Taylor, 1971; Stein et al., 1979). The characteristic property of weakly bound cross-bridges, aside from their low actin affinity (Stein et al., 1979; Chalovich et al., 1981), rapid kinetics for attachment and detachment to and from actin (Lymn and Taylor, 1971; Stein et al., 1979; Chalovich et al., 1981), and small calcium effect on affinity for the actin-tropomyosin-troponin complex (Chalovich et al., 1981; Wagner and Giniger, 1981), is their relative inability to cooperatively activate regulated actin (Chalovich et al., 1983). In contrast, force-generating (strongly binding) cross-bridges with higher actin affinity (Marston and Weber, 1975; White and Taylor, 1976; Highsmith, 1977; Margossian and Lowey, 1978; Greene and Eisenberg, 1980a; Greene et al., 1983), slower actin binding kinetics (White and Taylor, 1976; Marston, 1982; Konrad and Goody, 1982), and greater effect of calcium on their actin affinity (Greene and Eisenberg, 1980b), are characterized by their ability to cooperatively activate regulated actin (Bremel et al., 1972; Greene and Eisenberg, 1980b). Because of these distinctly different properties, it was assumed that the structure of a weakly bound actomyosin complex is different from that of a strongly bound complex, and it was proposed that force generation might result from a structural change associated with the transition from a weakly bound to a strongly bound actomyosin complex (White and Taylor, 1976; Eisenberg and Greene, 1980; Eisenberg and Hill, 1985). In this concept, weak cross-bridge attachment to actin is an essential precursor for force generation.

Indeed, it was recently shown (Brenner et al., 1991) that binding of caldesmon, an actin-binding protein of smooth muscle, inhibits the weak type of attachment of cross-bridges to actin in relaxed rabbit skeletal muscle fibers. This inhibition resulted in a parallel reduction of active force generation, even though the actin-binding fragments of caldesmon used in that study had no detectable effect on actin interaction of strongly binding cross-bridges (e.g., in the presence of PP_i at high $[Ca^{2+}]$ or under rigor conditions). Thus, this previous study supported the functional significance of the weakly bound cross-bridge as an attached, non-force-generating precursor of the force-generating cross-bridge.

However, that evidence was derived from experiments under low temperature and low ionic strength (μ) conditions. Thus, the question remained whether, at higher temperature and physiological ionic strength, weakly attached cross-bridges also exist in rabbit skeletal muscle and play a similar role in force generation. It was previously shown at physiological ionic strength (170 mM), but at low temperature, that relaxed fibers had detectable stiffness (Brenner et al.,

Received for publication 3 August 1994 and in final form 7 March 1995.

Address reprint requests to Dr. B. Brenner, Department of Clinical Physiology, Medical School Hannover, D-30623 Hannover, Germany.

Dr. Kraft's present address: National Institutes of Health, NIAMS, Bethesda, MD 20892. Tel: 301-496-5417; Fax: 301-402-0009; E-mail: tel@helix.nih.gov.

0006-3495/95/06/2404/15 $2.00

1986; Schoenberg, 1988). It remained, however, unclear whether that stiffness originated from attached cross-bridges or from non-cross-bridge structures. Furthermore, it was not ruled out that at more physiological temperatures weak cross-bridge binding to actin may no longer occur. Using actin-binding fragments of caldesmon to selectively inhibit weak cross-bridge binding to actin, we now report significant stiffness in relaxed fibers even for physiological ionic strength at high temperature. This stiffness apparently originates from weakly attached cross-bridges. The observed parallel inhibition of active force and relaxed fiber stiffness by caldesmon fragments at physiological conditions further supports the concept that cross-bridge attachment in a weak-type conformation is essential for the subsequent transition of the cross-bridges into force-generating states. In addition, our experiments show that the reduction of active force generation upon binding of caldesmon fragments to actin is not a result of changes in cross-bridge cycling kinetics.

A brief account of the present results was previously reported (Kraft et al., 1991).

MATERIALS AND METHODS

Proteins

Caldesmon was prepared from turkey gizzards by a modified method of Bretscher (1984). Actin-binding fragments of caldesmon were obtained by digestion of caldesmon with chymotrypsin (5 min at 25°C with 1:1000 (w/w) ratio of chymotrypsin to caldesmon). A mixture of three 20-kDa actin-binding fragments was isolated (Chalovich et al., 1992) and finally dialyzed against relaxing solution. Details of the properties of the 20-kDa fragments have been reported (Velaz et al, 1993).

Fiber preparation

Single chemically skinned fibers from rabbit psoas muscle were isolated according to a method described earlier (Brenner, 1983; Yu and Brenner, 1989). To prevent protein degradation, the skinning solution always contained several protease inhibitors (see composition of solutions below). To provide conditions similar to those in vivo, we replaced propionate by creatine phosphate for adjustment of ionic strength. Furthermore, to minimize oxidation of reactive groups within the proteins, we added glutathione (10 mM) to the skinning solution. We also isolated single fibers within a few hours after dissecting the muscle bundles and kept them as isolated fibers to reduce substrate depletion and diffusion problems. These precautions resulted in even better preservation of the mechanical stability of the muscle fibers than we previously achieved (Brenner, 1983). The fibers could easily be used for experiments including activation at high and low temperature even after 5 days of storage in the refrigerator without any detectable decrease in sarcomeric stability or force generation compared with freshly prepared fibers.

Solutions

All solutions were adjusted to pH 7.0 at the appropriate experimental temperature. The chemicals were obtained from Sigma Chemical Co., Munich, Germany, except where noted.

The skinning solution contained 5 mM KH_2PO_4, 3 mM magnesium acetate, 5 mM EGTA, 1 mM sodium ATP (Merck, Darmstadt, Germany), 50 mM sodium creatine phosphate, 5 mM NaN_3, 10 mM glutathione, 2 mM dithiothreitol, 100 μM (4-(2aminoethyl)-benzylsulfonyl-fluorid) (Calbiochem, La Jolla, CA), 1 μg/ml aprotinin, and 10 μM each leupeptin, antipain, E64, and pepstatin. Glutathione and the protease inhibitors were freshly added before using the solution. Immediately after dissection, the fiber bundles were incubated for 30 min at 5°C in skinning solution containing 0.5% Triton X-100. Before addition to the skinning solution, the Triton X-100 was equilibrated with an excess of the mixed bed resin AG 501-X8 (Bio-Rad Laboratories, Richmond, CA) to remove degraded material. After incubation in Triton X-100 containing skinning solution, the bundles were transferred to skinning solution without the detergent for isolation of single fibers.

The preactivating and activating solution contained 10 mM imidazole, 2 mM $MgCl_2$, 1 mM Mg-ATP, 2 mM dithiothreitol, 10 mM caffeine, 10 mM sodium creatine phosphate, 500 U/ml (Sigma) creatine phosphokinase, and 1 mM EGTA or 1 mM Ca-EGTA, respectively. The ionic strength was adjusted by adding sodium creatine phosphate.

The relaxing solution with Mg-ATP contained 10 mM imidazole, 2 mM $MgCl_2$, 1 mM EGTA, 1 mM Mg-ATP, and 1 mM dithiothreitol. The ionic strength was adjusted by adding sodium creatine phosphate.

The solutions with Mg-ATPγS, for low calcium concentrations, contained 10 mM imidazole, 2 mM $MgCl_2$, 3 mM EGTA, 10 mM Mg-ATPγS (Boehringer-Mannheim, Indianapolis, IN; purified by ion exchange chromatography as previously described in Kraft et al., 1992), 1 mM dithiothreitol, 0.2 mM Ap_5A, 0.5 U/ml hexokinase, and 200 mM glucose. For high calcium concentrations, the EGTA was replaced by 1 mM Ca-EGTA. For adjustment of ionic strength, sodium creatine phosphate was replaced by potassium propionate to avoid generation of ATP by endogenous creatine phosphokinase.

The rigor solution contained 10 mM imidazole, 150 mM potassium propionate, 2.5 mM EGTA, and 2.5 mM EDTA.

The solution with Mg-PP_i contained 10 mM imidazole, 2 mM $MgCl_2$, 1 mM Ca-EGTA, 4 mM Mg-PP_i, 1 mM dithiothreitol, 200 μM Ap_5A, and 140 mM potassium propionate.

The solution for measurements of isometric fiber ATPase under preactivating and activating conditions contained 20 mM imidazole, 2 mM $MgCl_2$, 3 mM EGTA or Ca-EGTA, respectively, 5 mM Mg-ATP, 10 mM caffeine, 0.25 mM Ap_5A, 5 mM NaN_3, 50 U/ml lactate dehydrogenase (Sigma), 250 U/ml pyruvate kinase (Sigma), 2 mM phosphoenol pyruvate, and approximately 0.2 mM NADH. The ionic strength was adjusted with potassium propionate. Phosphoenol pyruvate and pyruvate kinase served to follow fiber ATPase by coupling the rephosphorylation of ADP to the reduction of pyruvate to lactate by oxidation of NADH to NAD^+ and following the change in absorbance at 360 nm.

Equilibration and removal of caldesmon fragments

Unless otherwise stated, equilibration of the skinned fibers with the actin-binding fragments of caldesmon was allowed by incubation for 1 h in relaxing solution (ionic strength, 50 mM) to which the fragments were added. All solutions that were used subsequent to equilibration contained the same concentration of fragments as used for equilibration to avoid their untimely loss from the fibers. To ensure reversibility of effects on fiber mechanics, caldesmon fragments were removed from the fibers at the end of each experiment. Fibers were incubated for at least 30 min with calmodulin (0.2 mg/ml) in a Mg-PP_i solution with calcium (pCa 4.5). Binding of the caldesmon fragments to calcium-calmodulin reversed observed effects of the caldesmon fragments. Usually 90–100% of the initial fiber stiffness and force were restored. After very extended experiments, e.g., measurements of isometric fiber ATPase (see Fig. 8) at different caldesmon concentrations, the removal of caldesmon fragments restored only approximately 80% of original force and stiffness. This incomplete reversibility might not be a consequence of incomplete removal of the caldesmon fragments from actin but may rather be a result of some irreversible structural damage within the fiber during extended activation.

Confocal microscopy

Diffusion of caldesmon fragments into skinned fibers was followed by confocal microscopy. For this purpose, rhodamine-labeled caldesmon frag-

ments were prepared by modifying the protein with rhodamine X iodoacetamide (Molecular Probes, Eugene, OR). The actin-binding fragments of caldesmon were reduced by incubating with 10 mM dithiothreitol for 30 min at 37°C under a N_2 atmosphere. Excess dithiothreitol was removed on a 0.75- × 10-cm gel filtration column of ACA 202 (Spectrum, Los Angeles, CA) equilibrated with 100 mM NaCl, 50 mM Tris-HCl, pH 7.5, 1 mM EDTA, and 1 mM NaN_3. Subsequently, excess rhodamine X iodoacetamide was removed by gel filtration (Sephadex G-25, Pharmacia, Uppsala, Sweden). The elution buffer contained 10 mM imidazole, 2 mM $MgCl_2$, 1 mM EGTA, 1 mM dithiothreitol, and 34 mM potassium propionate.

Diffusion of rhodamine-labeled caldesmon fragments into skinned fibers was observed in relaxing solution. The labeled caldesmon fragments were also tested in mechanical experiments. As we found no difference in their inhibitory effect on the weak cross-bridge attachment compared with unlabeled caldesmon fragments, we included the data with the fluorescently labeled caldesmon fragments in the present results.

The system for confocal microscopy consisted of a Zeiss Axiophot fluorescence microscope, a Bio-Rad MRC-600 confocal scanner and a Silicon Graphics Personal Iris 4D/25 workstation with 32 megabytes of main memory (Silicon Graphics, Mountain View, CA). The images were recorded with a Zeiss Neofluar 40× N.A. 1.3 objective. The system was equipped with an argon/krypton mixed gas laser. Image processing was done on the Silicon Graphics workstation with Imaris (distributed by Bitplane, Technopark, Zürich, Switzerland), a three-dimensional multi-channel image processing software specialized for confocal microscopy.

For confocal microscopy, the fibers were mounted in a shallow (depth approximately 0.2 mm) flow-through chamber (total volume approximately 350 μl) mounted on a microscope slide and covered with a coverslip such that fibers were completely surrounded by solution (the chamber was kindly provided by M. Lezzi, ETH, Zürich, Switzerland). For adding the fluorescently labeled proteins quickly, new solution could be sucked through while the chamber remained mounted on the microscope stage.

Experimental protocol

In the mechanical set-up, the muscle fibers were mounted to the force transducer and the lever with Histoacryl (Braun, Melsungen, Germany). To stabilize the attached ends, fibers were transferred into rigor solution and approximately 0.5 mm of the fibers at each end was fixed with a 1% glutaraldehyde solution to which toluidine blue was added as an optical marker. The fixative was applied to the fiber ends by a micropipette, and the higher density of the glutaraldehyde/dye solution provided a rapid vertical flow that ensured quick removal of the fixative from the area surrounding the fiber (modified from Chase and Kushmerick, 1988). During activation, the striation pattern was stabilized by using the method described earlier (Brenner, 1983).

Isometric force and the rate constant of force redevelopment after a short period of isotonic shortening were determined according to the method described previously (Brenner and Eisenberg, 1986).

Isometric fiber ATPase was determined in a narrow slot-like chamber ($1.5 \times 2 \times 16$ mm^3) that was part of a circulating system. The incubating solution was circulated from the chamber through an analytical flow cell, a cooling unit, and back into the chamber. The flow cell was part of a fixed wavelength monitor (UV-M II, Pharmacia), where changes in absorption at 360 nm as a result of the decrease of NADH concentration were measured. The complete system had a volume of 120 μl, and the fiber length was between 10 and 15 mm. For each condition, the steady-state ATPase activity was recorded for at least 5 min. ATPase activity was expressed as relative activity by normalizing the observed slopes with respect to the slope recorded in the absence of caldesmon fragments.

The muscle chamber was designed such that, simultaneously with ATPase measurements, isometric force and the rate constant of force redevelopment after a short period of lightly loaded shortening and subsequent restretch to the original sarcomere length could be recorded with sarcomere length feedback (Brenner and Eisenberg, 1986). In addition, it was possible to monitor the structural integrity of the fiber by light microscopy.

To determine initial shortening velocity in the absence and presence of caldesmon fragments, we plotted the logarithm of instantaneous shortening velocity versus sarcomere length change (Brenner, 1980). Initial shortening velocity (v_i) was estimated by extrapolation of these linear plots back to the isometric sarcomere length (see Fig. 9).

Fiber stiffness was measured by applying ramp-shaped stretches to one end of the fibers. Apparent fiber stiffness was defined as the ratio of force increment over filament sliding when filament sliding had reached 2 nm/half-sarcomere (chord stiffness).

Stretch velocity could be varied from 10^{-1} to 5×10^4 (nm/half-sarcomere)/s to obtain stiffness-speed relations in the absence and presence of caldesmon fragments.

Data analysis

For each fiber, we first calculated the mean values of all data points obtained for identical conditions during the complete experimental run on that fiber. To summarize data from several fibers, we calculated average and standard deviation of the mean values determined for each individual fiber. Mathematical simulations were done with the KINSIM modeling program written by Barshop et al. (1983) and placed into microcomputer format by Dr. B. Plapp (University of Iowa).

RESULTS

Diffusion of the actin-binding caldesmon fragments

The series of images taken by confocal microscopy (Fig. 1) show that within less than 1 h constantly high fluorescence intensity is established throughout the whole fiber cross section. This indicates that equilibration with the 20-kDa caldesmon fragments has reached completion. This is consistent with our earlier findings obtained by recording fiber stiffness and equatorial x-ray diffraction patterns. In all experiments presented here, we therefore allowed 1 h for equilibration before studying effects of the caldesmon fragments.

Effect of caldesmon fragments on stiffness in and out of overlap

In the presence of caldesmon fragments, the stiffness of relaxed fibers decreases (Fig. 1), suggesting that, by binding to actin, caldesmon fragments reduce the number of cross-bridges bound weakly to actin. If the effect of caldesmon fragments is a result of a reduction of cross-bridge binding, the caldesmon fragments should have no effect on fiber stiffness if the fiber is stretched beyond overlap. This is demonstrated in Fig. 2*A*.

Inhibition of weak cross-bridge attachment to actin is expected to decrease fiber stiffness at all speeds of stretch by a similar percentage. Therefore we compared stiffness-speed relations of relaxed fibers in the presence and absence of caldesmon fragments. Fig. 2*B* shows that, within the scatter of the data, caldesmon fragments reduce fiber stiffness for all speeds of stretch by a similar fraction. As a consequence, for all following experiments, measurements of fiber stiffness were limited to a single speed of stretch of approximately 10^4 nm/half-sarcomere/s, instead of recording complete stiffness-speed relations.

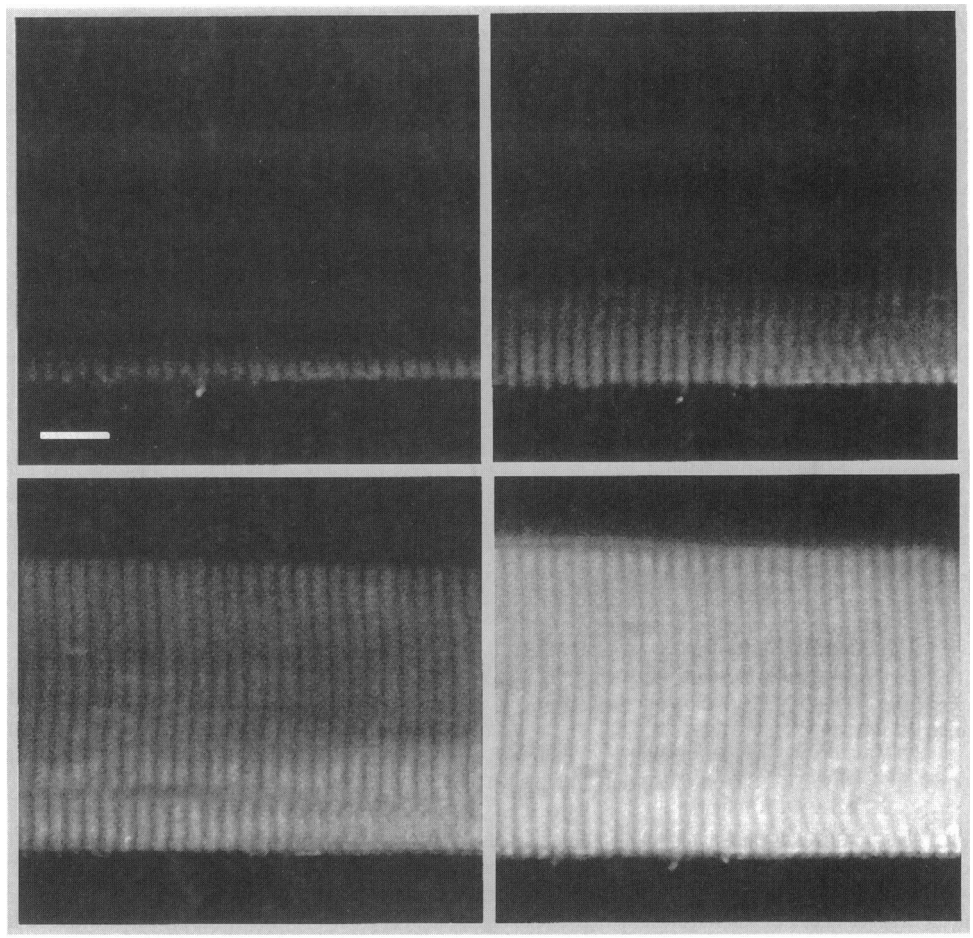

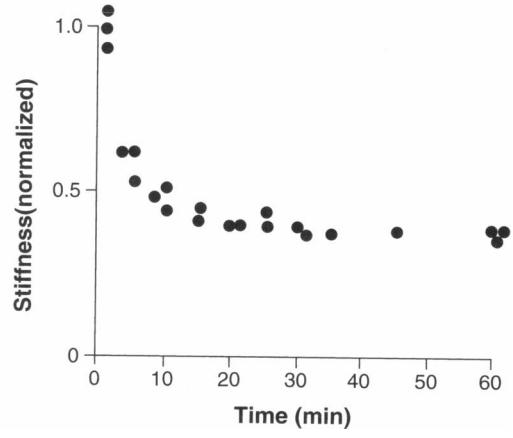

FIGURE 1 Confocal images of a skinned muscle fiber recorded during diffusion of 0.6 mg/ml rhodamine-labeled caldesmon fragment. Images show optical sections through middle of fiber. Fluorescence intensity reflects amount of fluorescently labeled protein in the examined optical section. Diffusion occurred under relaxing conditions at μ = 120 mM and 22°C; scale bar is 10 μm. Diffusion was followed in real time. Thus, a higher concentration of free fluorescently labeled caldesmon fragments was present within the fiber than was present after washing out free caldesmon. This accounts for the somewhat fuzzier structural details than those seen after washing out free caldesmon. Slower staining of upper part of fiber results from flowing caldesmon-containing solution in one direction (bottom to top) through the trough. Time of incubation: scanned during 1st min (upper left), 5th min (upper right), 10th min (lower left), and 30th min of incubation (lower right). The diagram shows the time course of diffusion of 0.4 mg/ml caldesmon fragment into skinned skeletal muscle fiber, monitored by inhibiting effect on relaxed fiber stiffness (μ = 50 mM). Effect was shown to be fully reversible (Brenner et al., 1991).

Reduction of relaxed fiber stiffness by caldesmon fragments at near physiological conditions

At physiological ionic strength, the relaxed fiber stiffness is low, making it difficult to distinguish cross-bridge-dependent stiffness from non-cross-bridge stiffness (cf. Brenner et al., 1986; Schoenberg, 1988). For example, as shown in Fig. 3, relaxed fiber stiffness at 5°C and μ = 170 mM is approximately 28% of that at 5°C and μ = 20 mM. This effect of ionic strength is smaller than previously reported (Brenner et al., 1986) as we now use the physiological anion creatine phosphate rather than chloride for adjusting the ionic strength. At μ = 20 mM and a speed of stretch of approximately 10^4 (nm/half-sarcomere)/s, fiber stiffness is approximately 42% of stiffness in rigor. Thus, stiffness observed at μ = 170 mM corresponds to approximately 8% of rigor stiffness. Increasing temperature from 5 to 20°C causes a reduction of relaxed fiber stiffness by approximately one-third such that the remaining stiffness of a relaxed fiber at 20°C and 170 mM ionic strength without caldesmon fragments is approximately 5–6% of rigor stiffness.

By examining the effect of caldesmon fragments, it is possible to show that at least part of the relaxed fiber stiffness

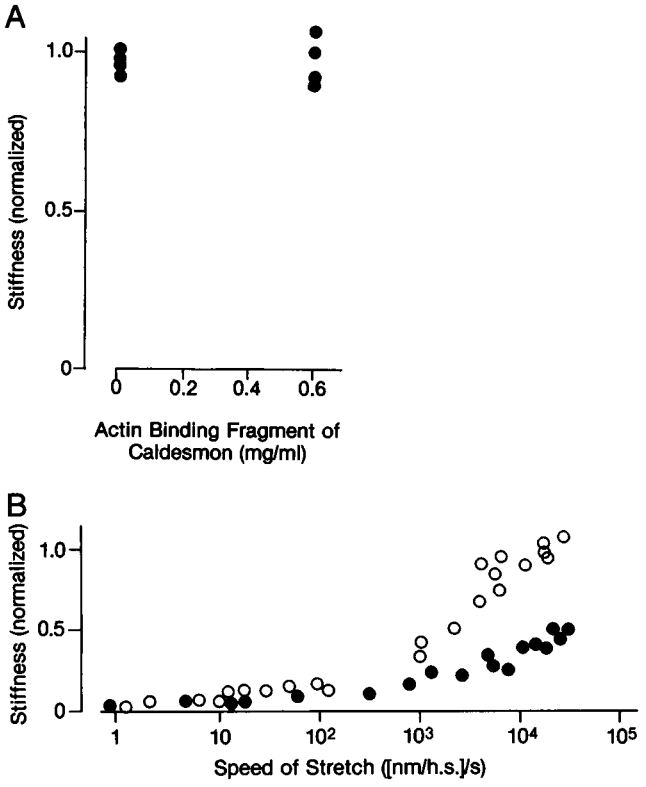

FIGURE 2 Effect of caldesmon fragments on relaxed stiffness of a fiber out of overlap (*A*) and at various speeds of stretch in normal overlap (*B*). All experiments were done at μ = 50 mM. Stiffness was normalized to that in the absence of caldesmon fragments at high stretching speed of approximately 10^4 nm/half-sarcomere/s. (*A*) Sarcomere length, 4.2 μm. (*B*) Sarcomere length, approximately 2.3 μm. Stiffness of relaxed fiber measured at various speeds of stretch before (○) and after (●) incubation with 0.8 mg/ml actin-binding caldesmon fragments.

is caused by cross-bridge binding. Under all conditions studied (170 mM, 5 and 20°C, Fig. 4; and 120 mM, 5°C and 20°C, data not shown), the diffusion of caldesmon fragments into the fibers caused a significant reduction in relaxed fiber stiffness. Equatorial x-ray diffraction patterns obtained from relaxed fibers under low and high ionic strengths at 5°C also showed a significant decrease in the intensity ratio I_{11}/I_{10} with increasing concentrations of caldesmon fragment (Kraft and Yu, unpublished data). These equatorial data indicate a shift of mass away from the thin filament region, consistent with a decrease in the fraction of attached cross-bridges.

Parallel inhibition of active force and relaxed fiber stiffness

Under all conditions examined in the present study, active force decreased in parallel with relaxed fiber stiffness as the concentration of caldesmon fragments was raised. Fig. 5 *A* shows examples from 170 mM ionic strength at different temperatures. Even at 30°C and 170 mM ionic strength, active force was significantly depressed by caldesmon fragments. This condition presented particular difficulties because of the instability of fully activated muscle fibers at

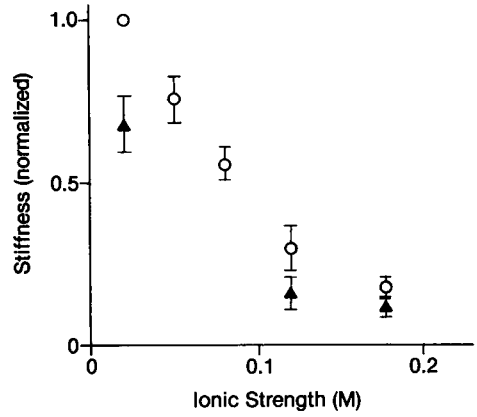

FIGURE 3 Relaxed fiber stiffness versus ionic strength at 5°C (○) and at 20°C (▲); n = 5–6 fibers. Values normalized with respect to stiffness at μ = 20 mM and 5°C. Ionic strength adjusted with sodium creatine phosphate. Relaxed fiber stiffness at μ = 20 mM and 5°C is approximately 42% of rigor stiffness. Note that raising temperature from 5 to 20°C reduces relaxed fiber stiffness by approximately 30%.

30°C. The protocol used was to first measure force in the presence of 0.6 mg/ml caldesmon fragments. As caldesmon fragments reduce active force even at this high temperature, a homogeneous sarcomeric structure was maintained over sufficiently long periods like those at 5°C. After removing the caldesmon fragments with calcium-calmodulin, force increased at least fourfold. This is an underestimate as structural instability at these high force levels may have lowered the force at full activation in the absence of caldesmon fragments. Nevertheless, these data indicate that the effects of caldesmon are qualitatively similar at 30, 20, and 5°C. Under all conditions, caldesmon fragments reduce active force by at least 75%.

Caldesmon fragments did not affect strong cross-bridge attachment to actin in the presence of Mg-PP_i at 20°C or

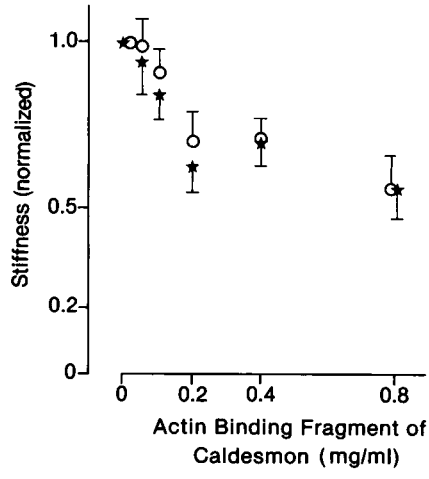

FIGURE 4 Stiffness of relaxed fibers versus concentrations of actin-binding caldesmon fragments; μ = 170 mM, at 5°C (○) and at 20°C (★); n = 7–9 fibers. All values were normalized to fiber stiffness in the absence of caldesmon fragments at 5 and 20°C, respectively.

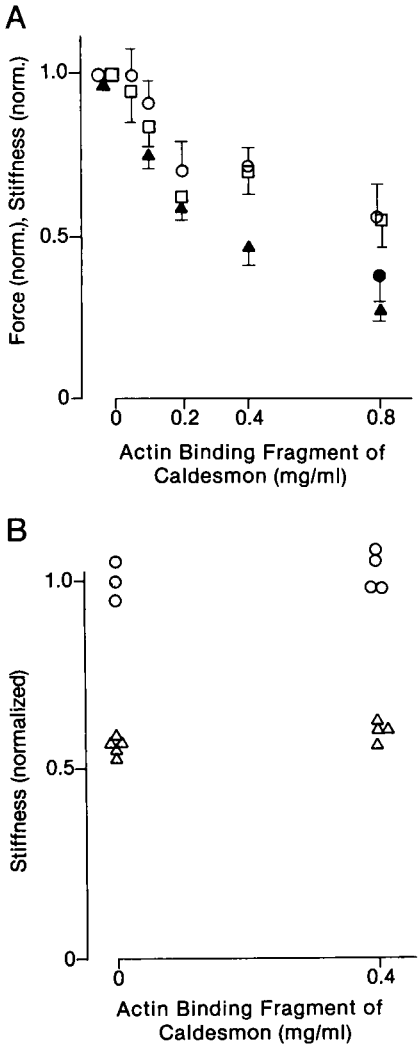

FIGURE 5 (*A*) Effect of caldesmon fragments on maximal isometric force at 5°C (▲) and at 20°C (●) and on relaxed fiber stiffness at 5°C (○) and at 20°C (□); μ = 170 mM; n = 7–9 fibers. (*B*) Shows fiber stiffness in the absence and in the presence of 0.4 mg/ml caldesmon fragments in rigor (○, 30°C) and in the presence of 4 mM Mg-PP_i (△, 20°C); μ = 170 mM. Values were normalized to rigor stiffness in the absence of caldesmon fragments.

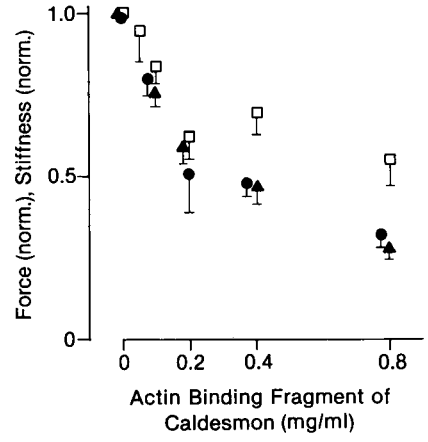

FIGURE 6 Inhibition of active force (▲), active stiffness (●), and relaxed stiffness (□) for increasing concentrations of caldesmon fragments at 5°C and μ = 170 mM. All data were normalized to force or fiber stiffness in the absence of caldesmon fragments; n = 4–7 fibers. Active stiffness without caldesmon fragments is 74% of rigor stiffness. Note that active force and active stiffness essentially change in proportion. This does not leave much room for large compliance in myofilaments under these conditions. This agrees with our previous data for partial activation under similar experimental conditions (Brenner, 1988).

under rigor conditions at 30°C (Fig. 5 *B*), at 20°C, or at 5°C (data not shown). Therefore, it appears to be the inhibition of weak cross-bridge binding to actin that is responsible for inhibition of active force.

Under all conditions shown in Fig. 5 *A*, caldesmon fragments decreased active force to a greater extent than relaxed fiber stiffness. One explanation for this observation could be that fiber stiffness is dominated by compliance in the myofilaments such that fiber stiffness is less affected by caldesmon fragments than active force. To test for this possibility, we compared active force with active fiber stiffness at increasing concentrations of caldesmon fragments. As shown in Fig. 6, inhibition of active fiber stiffness, different from relaxed fiber stiffness, very closely follows inhibition of active force.

As caldesmon fragments apparently do not interfere with strongly bound cross-bridges (e.g.. Mg-PP_i cross-bridges), the question arises whether the greater inhibition of cross-bridge attachment under activating conditions (Fig. 6) is a result of some difference in the binding of caldesmon fragments to actin at high Ca^{2+} concentrations.

To answer this question, we examined the effect of caldesmon fragments on fiber stiffness in the presence of Mg-ATPγS. Mg-ATPγS is a nucleotide analogue (Goody and Eckstein, 1971) for which the elementary cleavage step is approximately 500-fold slower than for Mg-ATP (Bagshaw et al., 1973), and the rate of Mg-ATPγS hydrolysis in fibers is not affected by Ca^{2+} concentration (Dantzig et al., 1988; Kraft et al., 1992). Even at high Ca^{2+} concentration, ATPγS maintains essentially all cross-bridges in a weakly binding conformation (Kraft et al., 1992). Fig. 7 shows that in the presence of Mg-ATPγS caldesmon fragments have a greater effect on fiber stiffness at high Ca^{2+} concentration. The difference in inhibition with and without calcium in the presence of Mg-ATPγS is similar to the difference between inhibition of relaxed and active fiber stiffness by caldesmon fragments (Fig. 6). These results indicate that caldesmon is a better inhibitor of weak cross-bridge binding to actin in the presence of Ca^{2+}, which might quite well be a result of some Ca^{2+}-dependent difference in the binding of the caldesmon fragments to actin.

Effect of caldesmon fragments on cross-bridge cycling kinetics

Effect on relation of isometric fiber ATPase versus force

Reduction of active force in the presence of caldesmon fragments could be explained solely by the inhibition of weak cross-bridge binding to actin. We further tested, however, whether changes in turnover kinetics could add to the inhibition of active force by caldesmon fragments.

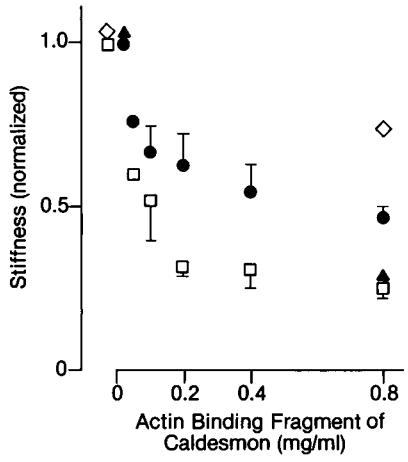

FIGURE 7 Decrease of fiber stiffness in the presence of 10 mM Mg-ATPγS at low [Ca^{2+}] (pCa 8), with μ = 75 mM (●) and 170 mM (◇), and high [Ca^{2+}] (pCa 4.5), with μ = 75 mM (□) and 170 mM (▲) at 1°C; n = 3–5 fibers. Data were normalized to respective values without caldesmon fragments. Note the difference in the extent of inhibition of fiber stiffness at low [Ca^{2+}] compared with that in the presence of 1 mM Mg-ATP (e.g., Fig. 6). This difference most likely is a result of the somewhat different experimental conditions for the Mg-ATPγS experiment (1°C, ionic strength adjusted by potassium propionate, 10 mM Mg-ATPγS versus 5°C, ionic strength adjusted by creatine phosphate, 1 mM Mg-ATP). Lower temperature and higher [Mg-ATPγS] were necessary to ensure saturation of myosin heads with Mg-ATPγS at the high [Ca^{2+}], switching to potassium propionate to avoid generation of ATP by native creatine kinase (Kraft et al., 1992).

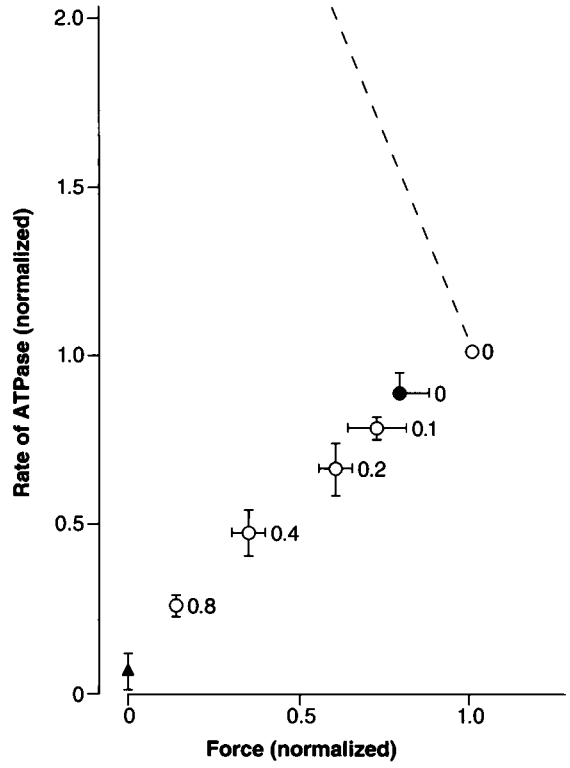

FIGURE 8 Isometric fiber ATPase versus isometric force at different caldesmon fragment concentrations. The number next to each symbol represents fragment concentration in milligrams per milliliter. μ = 170 mM at 5°C; n = 4 fibers. Both ATPase and force were normalized to their values in the absence of caldesmon fragments. Basal ATPase (▲) was determined under relaxing conditions. At the end of the experiment, caldesmon fragments were removed by calcium-calmodulin, and measurements were repeated (●); 80% of the initial force and 90% of the initial ATPase were restored. The dashed line (calculated values) represents the expected relation if the decrease in force with caldesmon fragments would mainly result from an increase in g_{app} (see Discussion).

One change that could cause a decrease in isometric force is an increase in the rate constant for the completion of the cross-bridge cycle, g_{app}. We used two different experimental approaches to study g_{app} in the presence and absence of caldesmon fragments.

Kushmerick and Krasner (1982) proposed that the ratio of isometric fiber ATPase over isometric force is proportional to g_{app} (g_{app} of the strained force-generating cross-bridge, i.e., g_1 in the notation of Huxley, 1957). If the decrease in active force is a result of a reduction in the number of cycling cross-bridges without a large change in g_{app}, fiber ATPase and active force should decrease in proportion upon addition of caldesmon fragments. To test for possible changes in g_{app}, we measured isometric fiber ATPase and the corresponding isometric force at different concentrations of caldesmon fragments.

We found (Fig. 8) that the decrease in active force is associated with a parallel decrease in ATPase activity, i.e., the ratio of ATPase over force is approximately the same for all force levels. Thus, binding of caldesmon fragments to actin apparently has no large effect on g_{app}.

Effect on isotonic shortening velocity

Maximal unloaded shortening velocity (v_i) is another parameter that is affected by g_{app} (g_{app} of unstrained or negatively strained cross-bridges, i.e., g_2 in the notation of Huxley, 1957). To study possible effects of caldesmon fragments on this parameter, shortening velocities at loads of approximately 6 and 15% of isometric force were measured and analyzed as described previously (Brenner, 1980). Fig. 9 shows that the binding of caldesmon fragments to actin has little if any effect on v_i. This suggests that caldesmon fragments do not alter the cross-bridge kinetics that determine the maximal speed of isotonic shortening. The slope of the curves increased in the presence of caldesmon fragments. This is consistent with the concept that a non-cross-bridge load inside the fiber (e.g., by elastic deformation of the cytoskeleton) is responsible for the slowing of shortening velocity with progressive fiber shortening. In the presence of caldesmon fragments, the postulated internal load, presumably induced by elastic deformation of cytoskeletal structures upon fiber shortening, has to be mastered by fewer active cross-bridges; i.e., in the presence of caldesmon fragments, additional loading of active cross-bridges with shortening increases more than in the absence of caldesmon fragments.

Effects of caldesmon fragments on force redevelopment at different levels of activation

The decrease in active force could also result from a decrease in the rate constant that characterizes the transition of cross-bridges into the force-generating, strongly binding states

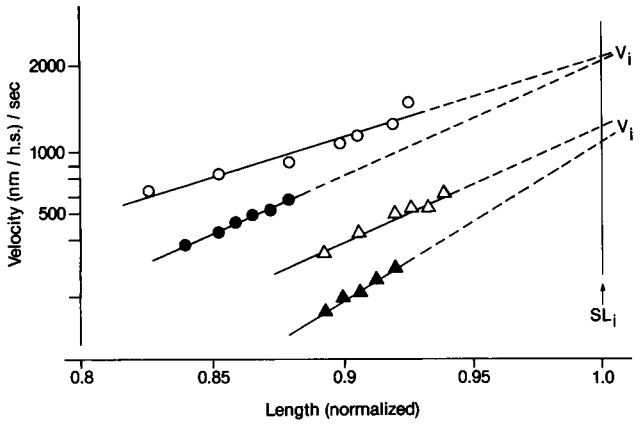

FIGURE 9 Length-velocity relations at two different external loads without caldesmon fragments (open symbols) and with 0.8 mg/ml actin-binding fragments (filled symbols). The slope of the relations results from the curvature of length trace recorded during isotonic shortening. Sarcomere length was normalized to initial (isometric) sarcomere length (SL_i). μ = 170 mM at 5°C; data are from one fiber. The different external loads were as follows: (○) 5.7% of maximal isometric force (F_{max}), no fragments; (△) 14.6% of F_{max}, no fragments; (●) 6.5% of F_{max}, 0.8 mg/ml actin-binding fragments; (▲) 15.5% of F_{max}, 0.8 mg/ml actin-binding fragments

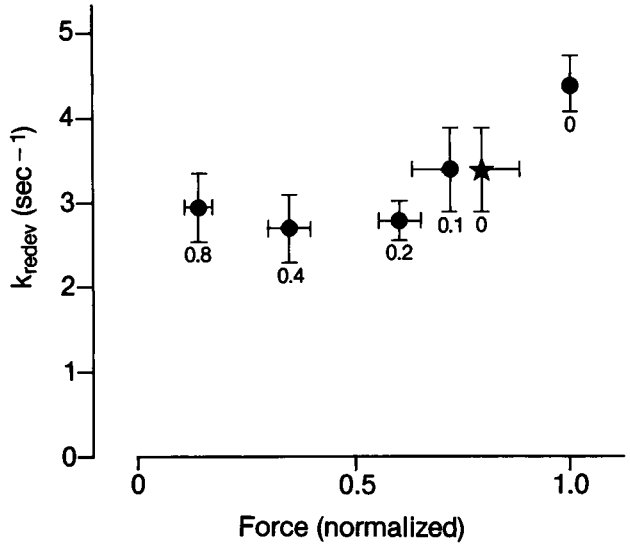

FIGURE 10 Rate constant of force redevelopment (k_{redev}) versus isometric force at different concentrations of caldesmon fragments. Values were taken from experiments in Fig. 8; therefore, the conditions are the same as for the ATPase measurements. μ = 170 mM at 5°C; n = 4 fibers. As in Fig. 8, k_{redev} was also determined after removal of caldesmon fragments at the end of the experiment (★), and 80% of initial force and approximately 75% of initial k_{redev} could be restored (see also Results).

(f_{app}). It has been demonstrated (Brenner, 1988) that the rate constant of force redevelopment after a period of unloaded shortening and subsequent restretch to the sarcomere length before shortening, k_{redev}, depends on f_{app} and g_{app} with k_{redev} = f_{app} + g_{app} (f^-_{app} assumed to be insignificant at low P_i concentrations). As we have now found that g_{app} is not significantly affected by caldesmon fragments, a decrease in k_{redev} would imply a decrease in f_{app}. As shown in Fig. 10, the results demonstrate that the reduction of isometric force to approximately 25% of F_{max} at 0.8 mg/ml caldesmon fragment concentration occurs with much smaller changes in k_{redev} (<33%). Moreover, there would be essentially no reduction in k_{redev} had the values of force and k_{redev} been compared with the values after removal of caldesmon fragments rather than with the initial values. Force and k_{redev}, however, decrease during prolonged activations such as those required for ATPase measurements. In a previous study, in which only short periods of activation were used, no change in k_{redev} was observed upon addition of caldesmon fragments.

DISCUSSION

We have now provided evidence that significant weak cross-bridge attachment to actin occurs in skinned fibers of the rabbit psoas muscle even at nearly physiological conditions, i.e., ionic strength of 170 mM and 20°C. Furthermore, weak cross-bridge attachment appears to be essential for force generation under all conditions studied, up to an ionic strength of 170 mM at temperatures as high as 30°C.

Extent of weak cross-bridge attachment to actin under physiological conditions

In skeletal muscle fibers of the rabbit, an increase in temperature from 5°C to more physiological values such as 20°C causes a decrease in relaxed fiber stiffness by approximately 30% at μ = 20 mM and measured at a high speed of stretch (10^4 nm/half-sarcomere/s; Fig. 3). This stiffness is still approximately one-third of rigor stiffness. If, at 20°C, the ionic strength is adjusted to more physiological conditions, such as 170 mM, relaxed fiber stiffness decreases to approximately 6% of rigor stiffness at the same speed of stretch. With the following assumptions, the apparent relaxed fiber stiffness indicates that at least 6% of all cross-bridges are weakly attached to actin under these near physiological relaxing conditions. (1) Essentially all cross-bridges are attached to actin in rigor (Cooke and Franks, 1980; Lovell and Harrington, 1981). (2) The stiffness of an attached cross-bridge is the same in rigor and under relaxing conditions. There is evidence, however, that the radial stiffness per cross-bridge under relaxing conditions is smaller than in rigor (Brenner and Yu, 1991; Xu et al., 1993b). If this also holds true for axial cross-bridge stiffness, then more than 6% of the cross-bridges are weakly attached. Furthermore, in our experiments, it was not possible to reach high enough stretch velocities at which fiber stiffness would be independent of the speed of stretch. Therefore, the fraction of weakly bound cross-bridges in relaxed fibers at 20°C and μ = 170 mM is most likely higher than 6%.

As for previous attempts to probe for weak cross-bridge attachment at high ionic strength but at 5°C (Brenner et al., 1986; Schoenberg, 1988), it could be argued that the relaxed fiber stiffness at high temperature and high ionic strength arises primarily from non-cross-bridge elements. However, our previously developed approach of probing for weak cross-bridge binding via inhibition by caldesmon fragments (Brenner et al., 1991) allows one to differentiate cross-bridge

from non-cross-bridge contributions to relaxed fiber stiffness. The observed extent of inhibition of relaxed stiffness suggests that at near physiological conditions a significant fraction (more than 50%) of the apparent stiffness of relaxed fibers is a result of cross-bridges that are weakly attached to actin. Using this approach to differentiate cross-bridge contributions from non-cross-bridge contributions by caldesmon, Granzier and Wang also concluded that a significant fraction of cross-bridges is weakly bound to actin at more physiological temperature in relaxed rabbit psoas muscle (Granzier and Wang, 1993).

We note that, under all conditions studied, neither relaxed fiber stiffness nor active force could be inhibited completely with caldesmon fragments. The remaining stiffness can be the result of different factors. First, caldesmon fragments do not completely block the sites for weak cross-bridge binding to actin; i.e., even in the presence of caldesmon fragments some cross-bridge interactions with actin may still be possible. This would also account for the approximately 25% of active force still seen at high caldesmon fragment concentrations. Second, there is nonhomogeneous binding of caldesmon fragments along the actin filaments. For example, preliminary data with confocal microcopy suggest that the binding of caldesmon fragments to actin is poorer near the Z-line. This question is currently under investigation.

Significance of weakly bound cross-bridges for force generation

In the present study, it is demonstrated that the binding of the 20-kDa fragments of caldesmon to actin causes parallel decrease in active force and relaxed fiber stiffness at physiological conditions as well as at low temperature and low ionic strength. As caldesmon fragments cannot inhibit the attachment of strongly binding cross-bridges to actin (Fig. 5 *B*), we conclude that active force is inhibited through inhibition of weak cross-bridge binding to actin; i.e., weak cross-bridge binding is an essential step to force generation. It should be pointed out that we are defining a weakly bound cross-bridge as one that does not activate the thin filament and has an actin affinity similar to that of a myosin head with ATP or ADP plus P_i (i.e., S1·ATP and S1·ADP-P_i states). The very similar inhibition of active stiffness and active force with that of relaxed fiber stiffness and stiffness in the presence of Mg-ATPγS at high Ca^{2+} concentration suggests that the essential state for inhibition has properties very similar to those that we refer to as weakly binding states. We are defining strong interactions as those that can activate the thin filament and have an actin affinity greater than or similar to that observed in the presence of Mg-PP_i. The state of the myosin head formed in the presence of Mg-PP_i is one of the lowest affinity states that significantly activates the thin filament (Greene and Eisenberg, 1988). Furthermore, to contribute to force generation, a cross-bridge must have an affinity at least this large; otherwise it would detach when strained upon force generation (Hill, 1974).

Our present and past data reveal several interesting points regarding the temperature dependence of cross-bridge behavior. Fig. 3 shows that an increase in temperature from 5 to 20°C results in a 30% reduction in the fraction of weakly bound cross-bridges whereas the active force increases approximately threefold (data not shown). This can be accounted for by a recent observation that in psoas fibers the increase in force with temperature is a result of an increase in the force generated by a cross-bridge while it occupies a force-generating state (Brenner, 1993) and is not a result of an increase in the number of cross-bridges occupying force-generating states. Another point of interest is that we observed that k_{redev} increases with temperature (Brenner, 1986) although we now show that the fraction of weakly bound cross-bridges decreases with increasing temperature. This means that the flux from the weakly bound cross-bridge states to the strongly bound states is not limited by the availability of weakly bound cross-bridges, unless weak binding is blocked by an inhibitor, as the rate of weak cross-bridge attachment is very fast (>1000s^{-1}). The twofold increase in k_{redev} from 5 to 15°C could be explained if the rate constant for P_i release is assumed to increase approximately threefold over this temperature range.

Inhibition of active force by caldesmon fragments is not a result of changes in cross-bridge turnover kinetics

Inhibition of active force may also result from changes in cross-bridge turnover kinetics upon binding of caldesmon fragments to actin. We tested this possibility by calculating the changes in turnover kinetics necessary to account for the observed inhibition of active force and comparing with experimental parameters that are sensitive to changes in cross-bridge turnover kinetics. The calculations were based on the equation $F \propto f_{app}/(f_{app} + g_{app})$ (Huxley, 1957; cf. Brenner, 1988) and on the values for f_{app} (3 s^{-1}) and g_{app} (1 s^{-1}) for rabbit psoas fibers at 5°C and μ = 170 mM (Brenner, 1986, 1988). To account for the decrease of isometric force in the presence of 0.8 mg/ml caldesmon fragments to approximately 25% of the initial isometric value, either f_{app} would have to decrease to less than 1/10 or g_{app} had to increase >10-fold. However, we did not observe changes in either g_{app} or f_{app} of this magnitude (cf. Figs. 8–10). A decrease in f_{app} by 30%, as may be derived from the change in k_{redev} (Fig. 10), would cause a decrease in force by no more than 10%. This is much less than the observed inhibition of force by approximately 75%.

Consideration of other possible mechanisms for inhibition of active force by caldesmon fragments

We observed that caldesmon fragments have much greater effects on the binding of myosin or myosin fragments to actin in the presence of ATP than in the presence of PP_i or ADP or in rigor, both in solution (Chalovich et al., 1987; Hemric & Chalovich, 1988) and in skinned rabbit psoas muscle fibers (Brenner et al., 1991, and present work). From these results, we suggested that caldesmon is a selective inhibitor of weak

cross-bridge binding to actin. This inhibition is selective as the affinity of caldesmon fragments for actin (approximately $5 \times 10^6\ M^{-1}\ s^{-1}$ at 50 mM ionic strength) is much greater than the affinity of S1·ATP to actin but is similar to the affinity of S1·ADP to actin. Also, under conditions for which strong cross-bridge binding to actin is unaffected by caldesmon fragments under equilibrium conditions, e.g., in the presence of Mg-PP_i, our data suggest that inhibition of the weak cross-bridge attachment is sufficient for inhibiting force production. This implies that production of force can occur only after mandatory attachment in a weakly binding configuration. In models of ATP hydrolysis by actomyosin similar to those proposed by Lymn and Taylor (1971) and Stein et al. (1979), the inhibition of active force and ATPase can be directly related to the ability of caldesmon fragments to inhibit actin attachment of the states preceding P_i release. If, as in these models, the states preceding P_i release are assumed to be weakly binding states, then the effectiveness of caldesmon fragments is readily explained.

More recent models of ATP hydrolysis incorporate a two-step binding of all myosin-nucleotide complexes to actin (Trybus and Taylor, 1980; Taylor, 1991; Geeves, 1989; Coates et al., 1985). Scheme 1 illustrates the two-step binding reaction of a myosin (M)-nucleotide (N) complex to actin (A).

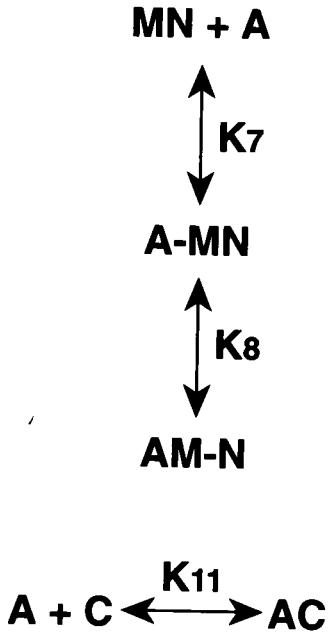

The rapid formation of a complex with low affinity to actin but high nucleotide affinity (A-MN) is followed by an isomerization to a complex that binds more strongly to actin and less tightly to the nucleotide (AM-N). In the presence of ATP, the isomerization is unfavorable ($K_8 < 1$) whereas, in the presence of ADP, the favorable isomerization ($K_8 \gg 1$) leads to an increase in the actin affinity of the complex. The tighter binding of S1·ADP to actin compared with S1·ATP is a result of a slightly larger K_7 and much larger K_8 (Taylor, 1991). As our studies suggest that a weakly bound intermediate must occur before force production, it is interesting to consider whether any A-MN intermediate (low affinity of the myosin head to actin) could fulfill this role or whether our results require assumption of a more classical type of weakly binding state such as M-ATP or M-ADP-P_i for which the subsequent isomerization (K_8) is unfavorable. If inhibition of force by caldesmon fragments is a result of inhibition of formation of any A-MN complex (low affinity for actin, see Scheme 1) then mathematical simulations of two-step binding schemes should show inhibition of turnover; i.e., force or ATPase activity, regardless of whether the pre-force-generating state is a weakly binding (small K_8) or strongly binding (large K_8) state.

Fig. 11*A* shows the simulated effect of caldesmon on the equilibrium binding of S-1 to actin, in the presence of ATP (a classical weakly binding state) and in the presence of ADP (a classical strongly binding state). Fig. 11 was produced by using the KINSIM modeling program (see Materials and Methods) and the equations in Scheme 1. These simulations are simplified and ignore any cooperative effects that occur as a result of the fact that caldesmon fragments might extend over more than one actin monomer. However, these simulations do provide examination of the general features of the inhibition. The simulations predict that caldesmon will inhibit the binding of S1·ATP to actin (both A-MATP plus AM-ATP), curve *b*, but will have little effect on the binding of S1·ADP to actin (A-MADP plus AM-ADP), curve *a*. Thus, even with the two-step binding of myosin to actin, caldesmon discriminates between the S1·ATP and S1·ADP type of complexes. It is important to note here that, at sufficiently high free caldesmon concentrations, the binding of S1·ADP to actin will also be inhibited. The important feature of these examples is the different sensitivity of the S1·ATP and S1·ADP complexes for competition by caldesmon.

The two-step binding of myosin to actin can be incorporated into a kinetic scheme for ATP hydrolysis. Scheme 2 shows a simplified model that incorporates activation of ATPase by binding of myosin to actin (actin activation of myosin ATPase).

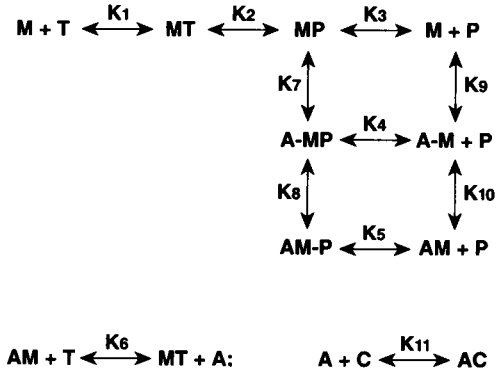

This actin activation results from an increase in the rate of product (P_i) release (i.e., $k_5 \gg k_3$) upon binding of myosin to actin. In this scheme, ATP and products (e.g., P_i) are represented by T and P, respectively. This model has intentionally been made

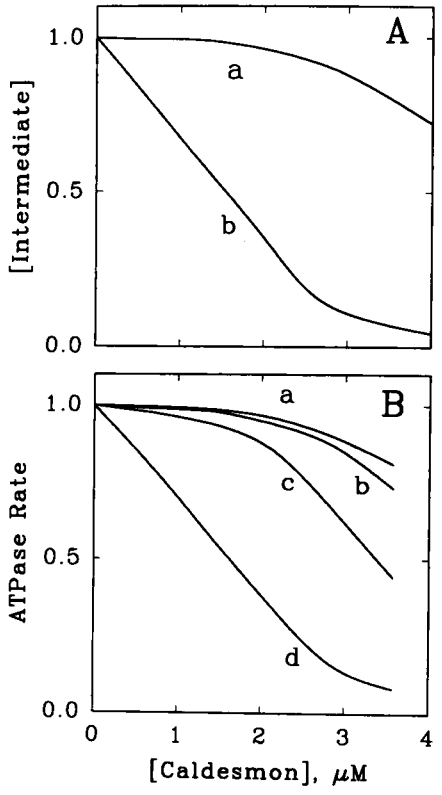

FIGURE 11 Simulation of effect of caldesmon on equilibrium binding (*A*) or on ATPase rate (*B*) of actin and S-1 (in solution). The protein concentrations used for simulations were 1 μM myosin, 20 μM actin, and 0 to 4 μM caldesmon. (*A*) Equilibrium binding. Binding intermediates in the presence of Mg-ATP and Mg-ADP are defined by Scheme 1 with K_7(ATP) = 4e3, K_7(ADP) = 4e4, K_8(ATP) = 1, K_8(ADP) = 100, and K_{11} = 3e6 M^{-1}. All results were normalized to values in the absence of caldesmon. (*B*) ATPase activity. Scheme 2 was modeled with the following equilibrium (K_n) and rate constants (k_n): $K_1 = 1 \times 10^{11}$ M^{-1} s^{-1}, $k_2 = 21$ s^{-1}, $k_{-2} = 7$ s^{-1}, $k_3 = 0.05$ s^{-1}, $k_{-3} = 0.2$ s^{-1}, $k_4 = 5$ s^{-1}, $k_{-4} = 20$ s^{-1}, $k_5 = 500$ s^{-1}, $k_{-5} = 2000$ s^{-1}, $k_6 = 1 \times 10^{10}$ s^{-1}, $k_{-6} = 1$ s^{-1}, $K_9 = 4 \times 10^4$, $K_{10} = 100$, and $K_{11} = 3 \times 10^6$ M^{-1} s^{-1}. Values for K_7 and K_8 were changed for different curves as follows: curve *a*, $K_7 = 40 \times 10^{-3}$ and $K_8 = 100$; curve *b*, $K_7 = 10 \times 10^{-3}$ and $K_8 = 400$; curve *c*, $K_7 = 4 \times 10^{-3}$ and $K_8 = 1000$; curve *d*, $K_7 = 4 \times 10^{-3}$ and $K_8 = 0.1$.

simple so that the effect of changing the pre-force-producing state from an S1·ATP-like state to an S1·ADP-like state can be examined. If the values of K_7 and K_8, the binding constants of the pre-force-generating state, are chosen to be characteristic of S1·ATP, then caldesmon is predicted to be an effective inhibitor of ATP hydrolysis. This simulation is shown in Fig. 11*B* (curve *d*). If values of K_7 and K_8 are those of an S1·ADP-like state, there is little inhibition of ATPase activity by caldesmon (curve *a*). Fig. 11*B* also shows the effects of varying K_7 and K_8. Curves *a*, *b*, and *c* show the effect of decreasing the value of K_7 with a proportionate increase in K_8 leaving the overall binding constant unchanged and high. In this case, even if the value of K_7 is identical with that of a typical S1·ATP state, caldesmon, in contrast to the experiment (e.g., Figs. 5–7), would be expected to inhibit active turnover much less effectively than binding to actin of an S1·ATP-like state (classical weakly binding state).

There is one difference between the modeling presented here and that of Geeves and co-workers. The simulations in Fig. 11 were done with equilibrium constants for K_7 and K_8 that are compatible with the work of Taylor (1991), Geeves (1989), and Coates et al. (1985). The rate constants k_7, k_{-7}, k_8, and k_{-8}, however, were derived from our stiffness data from skinned fibers (Brenner et al., 1986; Brenner, 1991; Kraft et al., 1992) and faster than those used by Geeves and colleagues. If the values of k_8 and k_{-8} are both reduced such that they become rate limiting in the ATPase cycle, then our simulations predict that caldesmon should inhibit the ATPase rate regardless of whether the state MP (see Scheme 2) is assumed to have properties similar to S1·ATP or S1·ADP. Such small values for both k_8 and k_{-8}, however, are incompatible with those derived from our stiffness-speed relations and therefore appear unrealistic.

It is important to note that this modeling was done with binding constants and protein concentrations used in solution studies. The concentration of caldesmon fragments at which 50% inhibition of a classical weakly binding state occurs while inhibition of a classical strongly binding is <10% very much depends on the assumed concentrations of actin and myosin. For instance, assuming an actin concentration of 380 μM and a myosin subfragment-1 concentration of 220 μM, 50% inhibition of a classical weakly binding state requires approximately 40 μM of caldesmon fragments. This is closer to the situation observed in muscle fibers. It has to be considered, however, that the effective actin and myosin head concentrations in muscle depend on geometrical constraints in the structured contractile system such that our present modeling cannot provide a definite prediction about the caldesmon concentrations needed in muscle for some 50% inhibition of a weak-type interaction. Nevertheless, this modeling shows that, in both conventional kinetic schemes (e.g., Lymn and Taylor, 1971; Stein et al., 1979) or kinetic schemes involving two-step binding for all myosin nucleotide states (Trybus and Taylor, 1980; Taylor, 1991; Geeves, 1989; Coates et al., 1985), caldesmon is an effective inhibitor of actin-activated myosin ATPase only when there is mandatory attachment of a state that has properties similar to an S1·ATP or S1·ADP-P_i state (e.g., overall affinity $\leq$0.1% of the affinity of force-producing states) and from which progress in the cycle (i.e., P_i release sequence) becomes faster upon binding of myosin to actin.

Implications for force generation

On the basis of the findings that in solution weakly associated actomyosin complexes have distinctly different properties compared with the strongly associated complex, it was previously assumed that weakly and strongly associated actomyosin complexes are structurally different. The change in the structure of the actomyosin complex, assumed to be associated with the transition from a weakly bound to a strongly bound cross-bridge, was proposed to be a major mechanism in force generation (White and Taylor, 1976; Eisenberg and Greene, 1980; Eisenberg and Hill, 1985).

One of the basic assumptions in this concept is that weak cross-bridge binding is an essential precursor for force gen-

eration. Our present data provide support for this assumption for all conditions studied, including physiological ionic strength at temperatures as high as 30°C.

Evidence for the assumed structural differences between weakly and strongly associated actomyosin cross-bridges was revealed by several structural studies. These studies have identified differences not only between the weakly associated actomyosin complex and the strongly bound rigor cross-bridge (Craig et al., 1985; Yu and Brenner, 1989; Walker et al., 1994; however, see also Pollard et al., 1993) but also between the weakly bound cross-bridge and the force-generating cross-bridge in active muscle by equatorial diffraction studies (Brenner and Yu, 1993) and resistance to osmotic compression (Brenner and Yu, 1991; Xu et al., 1993a,b).

Although the nature of these structural differences has not yet been fully determined, it is clear that the weak binding is site specific. Weak binding to actin is stoichiometric (Chalovich, 1992), and caldesmon and its fragments are thin thread-like molecules and yet cause very effective inhibition of weak cross-bridge binding to actin. On the other hand, the weak attachment may not have well defined steric orientations (nonstereospecific). Equatorial intensities and myosin layer lines indicate that weak cross-bridge binding to actin does not greatly alter the distribution of cross-bridge mass from a myosin-based distribution around and along the thick filaments (Matsuda and Podolsky, 1984; Yu and Brenner, 1989; Xu et al., 1994). Furthermore, probes placed on the myosin heads indicate that weakly attached cross-bridges have orientational disorder and high mobility (Fajer et al., 1991; Berger et al., 1989). Thus, although weak binding is site specific, it appears, in contrast to the strong cross-bridge binding, to be nonstereospecific.

On the basis of recent modeling of the crystallographic structure of myosin subfragment-1 (Rayment et al., 1993a) and the atomic model of the actin filament (Holmes et al., 1990) into the envelope provided by cryoelectron microscopy of decorated actin filaments (Milligan et al., 1990; Schröder et al., 1993), Rayment et al. (1993b) and Schröder et al. (1993) proposed that the weak cross-bridge binding to actin may originate from an interaction between the highly charged flexible NH_2 terminus of actin and the highly charged flexible loop between residues Tyr626 and Gln647 of myosin. The strong, force-producing interaction was proposed to involve additional regions of contact that are less flexible and that involve both hydrophobic and electrostatic interactions (Rayment et al., 1993b, Schröder et al., 1993). It is, however, as yet unclear whether in the presence of Ca^{2+} weak interactions form additional, electrostatic contacts that may account for the observed Ca^{2+} effects on actin-binding kinetics of the cross-bridge in the presence of the ATP analogue ATPγS. Although weakly binding properties (no activation of the thin filament; increase in actin affinity of at most two- to fourfold) are retained, the association and dissociation kinetics of the ATPγS-cross-bridge to and from actin are slowed almost 100-fold by Ca^{2+} (Kraft et al., 1992). Nevertheless, the interactions proposed by Rayment et al. (1993b) and Schröder et al. (1993) would readily account for the different binding properties of weak and strong interactions observed in solution and fibers, e.g., actin affinity and its ionic strength sensitivity and nonstereospecificity, and confirm the concept of distinct structural differences between weakly and strongly associated actomyosin complexes.

Thus, experimental evidence has been gathered for major assumptions that form the basis of the concept of force generation being associated with the transition from a weakly to a strongly bound cross-bridge.

Relation to the mechanism of force generation proposed by Huxley and Simmons (1971)

Despite this evidence, it may still be possible that the main contribution to generation of force occurs subsequent to the transition into the strongly bound states, analogous to the concept of Huxley and Simmons (1971). They assumed that isometric force generation results mainly from the same elementary mechanism that in their concept is responsible for the quick tension recovery that occurs when active tension has been reduced by a small stepwise length release of the muscle. This quick tension recovery was assumed to result from one transition or a sequence of transitions between several sterically well defined (stable) configurations of the actomyosin cross-bridge. In the concept of Huxley and Simmons (1971), isometric force results primarily from those cross-bridges that have undergone at least the first transition in the proposed sequence of rapidly reversible steps; i.e., isometric force is essentially generated by cross-bridges occupying the second (or a subsequent) state of the assumed series of sterically well defined (stable) states. The transition from possible weakly bound states to the first sterically well defined state in this concept is essentially insignificant for isometric force, and only little if any contribution to force is made by cross-bridges in the first of these structurally stable states (see below). However, when testing this concept with mechanical experiments, it was found (Brenner, 1991, 1993) that, not only under low but also under high temperature conditions, almost all isometric force (>80%) is generated before cross-bridges undergo even the first of the series of rapidly reversible reaction steps postulated by Huxley and Simmons to underlie quick tension recovery. This suggests that isometric force results from a structural change associated with a reaction step before and different from those proposed by Huxley and Simmons (1971).

In the modeling of Huxley and Simmons (1971) the contribution of the first stable state to isometric force is 25%. This results from an assumed average strain of 4 nm for cross-bridges in this first state. This assumption was necessary to account for the experimentally observed y_o value of 8 nm and the 12 nm and for the assumed intercept of the T_2 curve with the abscissa that reflects the strain in state 2. y_o is the necessary amplitude of filament sliding that drops isometric force to zero. In the modeling of Huxley and Simmons, y_o is the average strain in state 1 (4 nm) and state 2 (12 nm) with equal occupancy of both states. More recent

measurements of the y_0 value yielded only approximately 5 nm (e.g., Ford et al., 1977) whereas the T_2 intercept remained unchanged. To account for this much smaller value within the framework proposed by Huxley and Simmons (1971), the average strain of cross-bridges in state 1 has to be much less than 4 nm. Consequently, contribution to isometric force by cross-bridges in the first state, in this concept, should be much less than 25%.

Together with the observations that weak cross-bridge binding to actin is an essential step in force generation and that a weakly bound actomyosin cross-bridge in relaxed muscle has a significantly different structure from a force-generating cross-bridge in active muscle (Brenner and Yu, 1993), an alternative to the concept of Huxley and Simmons (1971) or of Eisenberg and Greene (1980) for generation of isometric force emerges (see Brenner et al., 1995). (In their 1980 proposal, Eisenberg and Greene assumed that the structural changes proposed by Huxley and Simmons to underlie quick tension recovery are associated with the transition from a weakly bound actomyosin cross-bridge to a strongly bound cross-bridge and that this structural change is the major mechanism for force generation. I.e., Eisenberg and Greene, in analogy to Huxley and Simmons (1971), also proposed that the major mechanism for generation of isometric force is the same as that assumed to mainly underlie quick tension recovery.) The alternative concept is that generation of isometric force occurs before and through reaction steps other than quick tension recovery, e.g., through the changes in the structure of the attached cross-bridge associated with the transition from a weakly to a strongly bound actomyosin complex. Subsequent reaction steps that are thought to underlie quick tension recovery are favored only in response to releases or during shortening of muscle.

If the weak binding occurs through the flexible NH_2 terminus of actin and the flexible loop within the myosin head (Rayment et al., 1993b; Schröder et al., 1993), there may be, averaged over all cross-bridges, no net strain in the weakly attached cross-bridge despite the mismatch between the periodicities of the thick and thin filaments. However, the transition into the stereospecific, force-generating strong interaction could result in a net average strain of the attached cross-bridges that, under isometric conditions, would turn into the driving force between the myofilaments. Because of the structural asymmetry in the actin filament, for each attached cross-bridge the structural change associated with the transition from the weak to the strong interaction could have a component in shortening direction. The magnitude of this component, however, may vary from cross-bridge to cross-bridge, a result of the mismatch between actin and myosin periodicity. The states that were proposed by Huxley and Simmons to mainly contribute to isometric force, in our concept, become significantly populated only in response to releases (quick tension recovery) and during fiber shortening.

This view is consistent with x-ray diffraction studies that suggest that structural changes of the attached cross-bridge associated with isometric force generation are associated with changes in equatorial intensities even when the fraction of attached cross-bridges remains essentially unchanged (Brenner and Yu, 1993). In contrast, structural changes associated with quick tension recovery do not affect equatorial intensities (Huxley et al., 1983; Irving et al., 1992). This could be accounted for if quick tension recovery results from a structural change within the attached actomyosin cross-bridge similar to that proposed by Rayment et al. (1993b). Our modeling shows that such a change would not significantly affect the low angle equatorial intensities (Malinchik and Yu, 1994).

In conclusion, our data show that, first, under a wide range of conditions, significant numbers of cross-bridges are weakly attached to actin in relaxed muscle. Second, force can always be inhibited through inhibition of this weak attachment. This indicates that weak cross-bridge binding to actin is an essential intermediate on the path to force generation. Third, a substantial body of evidence suggests that a major factor for generation of isometric force is the structural change in the actomyosin complex associated with the transition from a weakly bound to a strongly bound cross-bridge configuration. Transitions among strongly bound force-generating states become favored only in response to rapid releases (quick tension recovery) and during movement.

The authors thank Drs. J. C. Perriard, M. Messerli, and T. Wallimann, as well as B. Rothen-Rutishauser (Institute of Cell Biology, ETH, Zürich, Switzerland), for providing access to their confocal microscope and help with data collection and analysis. We also thank Dr. Bryce Plapp, Department of Biochemistry, University of Iowa, for providing a copy of the KINSIM modeling program in microcomputer format.

This work was supported by grants of the DFG to B.B. (Br 849/1–4), National Institutes of Health grant AR40540 to J.M.C, and a Nato Collaborative Research grant 930448.

REFERENCES

Bagshaw, C. R., J. F. Eccleston, D. R. Trentham, and D. W. Yates. 1973. Transient kinetic studies of the Mg^{++}-dependent ATPase of myosin and its proteolytic subfragments. *Cold Spring Harbor Symp. Quant. Biol.* 37:127–135.

Barshop, B. A., R. F. Wrenn, and C. Frieden. 1983. Analysis of numerical methods for computer simulation of kinetic processes: development of KINSIM–a flexible, portable system. *Anal. Biochem.* 130:134–145.

Berger, C. L., E. C. Svensson, and D. D. Thomas. 1989. Photolysis of a photolabile precursor of ATP (caged ATP) induces microsecond rotational motions of myosin heads bound to actin. *Proc. Natl. Acad. Sci. USA.* 86:8753–8757.

Bremel, R. D., and A. Weber. 1972. Cooperation within actin filament in vertebrate skeletal muscle. *Nature.* 238:97–101.

Brenner, B. 1980. Effect of free sarcoplasmic Ca^{2+} concentration on maximum unloaded shortening velocity: measurements of single glycerinated rabbit psoas muscle fibers. *J. Muscle Res. Cell Motil.* 1:409–428.

Brenner, B. 1983. Technique for stabilizing the striation pattern in maximally calcium-activated skinned rabbit psoas fibers. *Biophys. J.* 41: 99–102.

Brenner, B. 1986. The cross-bridge cycle in muscle: mechanical, biochemical and structural studies to characterize cross-bridge kinetics in muscle for correlation with the actomyosin ATPase in solution. *Basic Res. Cardiol.* 81,1:1–15.

Brenner, B. 1988. Effect of Ca^{2+} on cross-bridge turnover kinetics in skinned single rabbit psoas fibers: implications for regulation of muscle contraction. *Proc. Natl. Acad. Sci. USA.* 85:3265–3269.

Brenner, B. 1991. Dynamic dissociation and reassociation of actomyosin cross-bridges during force generation. A newly observed facet of cross-bridge action in muscle. *Proc. Natl. Acad. Sci. USA.* 88:10490–10494.

Brenner, B. 1993. Rapid dissociation and reassociation of force-generating cross-bridges. Effects of temperature and inorganic phosphate. *Biophys. J.* 64:250*a*. (Abstr.)

Brenner, B., J. M. Chalovich, L. E. Greene, E. Eisenberg, and M. Schoenberg. 1986. Stiffness of skinned rabbit psoas fibers in Mg-ATP and Mg-PP_i solutions. *Biophys. J.* 50:685–691.

Brenner, B., J. M. Chalovich, and L. C. Yu. 1995. Distinct molecular processes associated with isometric force generation and with rapid tension recovery after quick release. *Biophys. J.* In press.

Brenner, B., and E. Eisenberg. 1986. The rate of force generation in muscle: correlation with actomyosin ATPase in solution. *Proc. Natl. Acad. Sci. USA.* 83:3542–3546.

Brenner, B., and L. C. Yu. 1991. Characterization of radial force and radial stiffness in Ca^{2+}-activated skinned fibers of the rabbit psoas muscle. *J. Physiol.* 441:703–718.

Brenner, B., and L. C. Yu. 1993. Structural changes in the actomyosin cross-bridges associated with force generation. *Proc. Natl. Acad. Sci. USA.* 90:5252–5256.

Brenner, B., L.C. Yu, and J. M. Chalovich. 1991. Parallel inhibition of active force and relaxed fiber stiffness in skeletal muscle by caldesmon: implications for the pathway to force generation. *Proc. Natl. Acad. Sci. USA.* 88:5739–5743.

Bretscher, A. 1984. Smooth muscle caldesmon: rapid purification and F-actin cross-linking properties. *J. Biol. Chem.* 259:12873–12880.

Chalovich, J. M. 1992. Actin mediated regulation of muscle contraction. *Pharmacol. and Ther.* 55:95–148.

Chalovich, J. M., J. Bryan, C. E. Benson, and L. Velaz. 1992. Localization and characterization of a 7.3-kDa region of caldesmon which reversibly inhibits actomyosin ATPase activity. *J. Biol. Chem.* 267:16644–16650.

Chalovich, J. M., P. B. Chock, and E. Eisenberg. 1981. Mechanism of action of troponin and tropomyosin. *J. Biol. Chem.* 256:575–578.

Chalovich, J. M., P. Cornelius, and C. E. Benson. 1987. Caldesmon inhibits skeletal actomyosin subfragment-1 ATPase activity and the binding of myosin subfragment-1 to actin. *J. Biol. Chem.* 262:4885–4889.

Chalovich, J. M., L. E. Greene, and E. Eisenberg. 1983. Crosslinked myosin subfragment 1: a stable analogue of the subfragment ATP complex. *Proc. Natl. Acad. Sci. USA.* 80:4909–4913.

Chase, P. B., and M. J. Kushmerick. 1988. Effects of pH on contraction of rabbit fast and slow skeletal muscle fibers. *Biophys. J.* 53:935–946.

Coates, J. H., A. H. Criddle, and M. A. Geeves. 1985. Pressure-relaxation studies of pyrene-labeled actin and myosin subfragment 1 from rabbit skeletal muscle. *Biochem. J.* 232:351–356.

Cooke, R., and K. Franks. 1980. All myosin heads form bonds with actin in rabbit rigor skeletal muscle. *Biochemistry.* 19:2265–2269.

Craig, R., L. E. Greene, and E. Eisenberg. 1985. Structure of the actin-myosin complex in the presence of ATP. *Proc. Natl. Acad. Sci. USA.* 82:3247–3251.

Dantzig, J. A., J. W. Walker, D. R. Trentham, and Y. E. Goldman. 1988. Relaxation of muscle fibers with adenosine 5′-[γ-thio]triphosphate (ATP-[γS]) and by laser photolysis of caged ATP[γS]: evidence for Ca^{2+}-dependent affinity of rapidly detaching zero-force cross-bridges. *Proc. Natl. Acad. Sci. USA.* 85:6716–6720.

Eisenberg, E., and L. E. Greene. 1980. The relation of muscle biochemistry to muscle physiology. *Annu. Rev. Physiol.* 42:293–309.

Eisenberg, E., and T. L. Hill. 1985. Muscular contraction and free energy transduction in biological systems. *Science.* 227:999–1006.

Fajer, P. G., E. A. Fajer, M. Schoenberg, and D. D. Thomas. 1991. Orientational disorder and motion of weakly attached crossbridges. *Biophys. J.* 60:642–649.

Ford, L. E., A. F. Huxley, and R. M. Simmons. 1977. Tension responses to sudden length change in stimulated frog muscle fibres near slack length. *J. Physiol. (Lond.)* 269:441–515.

Geeves, M. A. 1989. Dynamic interaction between actin and myosin subfragment 1 in the presence of ADP. *Biochemistry.* 28:5864–5871.

Goody, R. S., and F. Eckstein. 1971. Thiophosphate analogs of nucleoside di- and triphosphates. *J. Am. Chem. Soc.* 93:6252–6257.

Granzier, H. L. M., and K. Wang. 1993. Passive tension and stiffness of vertebrate skeletal and insect flight muscles: the contribution of weak cross-bridges and elastic filaments. *Biophys. J.* 65:2141–2159.

Greene, L. E., and E. Eisenberg. 1980a. Dissociation of the actin subfragment-one complex by adenyl-5′yl imidodiphosphate, ADP, and PP_i. *J. Biol. Chem.* 255:543–548.

Greene, L. E., and E. Eisenberg. 1980b. Cooperative binding of myosin subfragment-1 to the actin-troponin-tropomyosin complex. *Proc. Natl. Acad. Sci. USA.* 77:2616–2620.

Greene, L. E., and E. Eisenberg. 1988. Relationship between regulated actomyosin ATPase activity and cooperative binding of myosin to regulated actin. *Cell Biophys.* 12:59–71.

Greene, L. E., J. R. Sellers, E. Eisenberg, and R. S. Adelstein. 1983. Binding of gizzard smooth muscle myosin subfragment-one to actin in the presence and absence of ATP. *Biochemistry.* 22:530–535.

Hemric, M. E., and J. M. Chalovich. 1988. Effect of caldesmon on the ATPase activity and the binding of smooth and skeletal myosin subfragments to actin. *J. Biol. Chem.* 263:1878–1885.

Highsmith, S. 1977. The effects of temperature and salts on myosin subfragment-1 and F-actin association. *Arch. Biochem. Biophys.* 180: 404–408.

Hill, T. L. 1974. Theoretical formalism for the sliding filament model of contraction of striated muscle. *Prog. Biophys. Mol. Biol.* 28:267–340.

Holmes, K. C., D. Popp, W. Gebhard, and W. Kabsch. 1990. Atomic model of the actin filament. *Nature.* 347:44–49.

Huxley, A. F. 1957. Muscle structure and theories of contraction. *Prog. Biophys.* 7:255–318.

Huxley, A. F., and R. M. Simmons. 1971. Proposed mechanism of force generation in striated muscle. *Nature.* 233:533–538.

Huxley, H. E., R. M. Simmons, A. R. Faruqi, M. Kress, J. Bordas, and M. H. J. Koch. 1983. Changes in the x-ray reflections from contracting muscle during rapid mechanical transients and their structural implications. *J. Mol. Biol.* 169:469–506.

Irving, M., V. Lombardi, G. Piazzesi, M. A. Ferenczi. 1992. Myosin head movement are synchronous with the elementary force-generating process in muscle. *Nature.* 357:156–158.

Konrad, M., and R. S. Goody. 1982. Kinetic and thermodynamic properties of the ternary complex between F-actin, myosin subfragment 1 and adenosine 5′-[,γ imido]triphosphate. *Eur. J. Biochem.* 128:547–555.

Kraft, T., J. M. Chalovich, L. C. Yu, and B. Brenner. 1991. Weak cross-bridge binding is essential for force generation. Evidence at near physiological conditions. *Biophys. J.* 59:375*a*. (Abstr.)

Kraft, T., L. C. Yu, H. J. Kuhn, and B. Brenner. 1992. Effect of Ca^{2+} on weak cross-bridge interaction with actin in the presence of adenosine 5′-[γ-thio]triphosphate. *Proc. Natl. Acad. Sci. USA.* 89:11362–11366.

Kushmerick, M. J., and B. Krasner. 1982. Force and ATPase rate in skinned skeletal muscle fibers. *Fed. Proc.* 41:2232–2237.

Lovell, S. J., and W. F. Harrington. 1981. Measurement of the fraction of myosin heads bound to actin in rabbit skeletal myofibrils in rigor. *J. Mol. Biol.* 149:659–674.

Lymn, R. W., and E. W. Taylor. 1971. Mechanism of adenosine triphosphate hydrolysis by actomyosin. *Biochemistry.* 10:4617–4624.

Malinchik, S., and L. C. Yu. 1994. Studies of the configurations of weakly attached and force-generating cross-bridges. Modeling of equatorial x-ray diffraction patterns. *Biophys. J.* 66:190*a*. (Abstr.)

Margossian, S. S., and S. Lowey. 1978. Interaction of myosin subfragments with F-actin. *Biochemistry.* 17:5431–5439.

Marston, S. B. 1982. The rates of formation and dissociation of actin-myosin complexes. *Biochem. J.* 230:453–460.

Marston, S. B., and A. Weber. 1975. The dissociation constant of the actin-heavy meromyosin subfragment-1 complex. *Biochemistry.* 14: 3868–3873.

Matsuda, T., and R. J. Podolsky. 1984. X -ray evidence for two structural states of the actomyosin cross-bridge in muscle fibers. *Proc. Natl. Acad. Sci. USA.* 81:2364–2368.

Milligan, R. A., M. Whittaker, and D. Safer. 1990. Molecular structure of F-actin and location of surface binding sites. *Nature.* 348:217–221.

Pollard, T. D., D. Bhandari, P. Maupin, D. Wachsstock, and A. G. Weeds. 1993. Direct visualization by electron microscopy of the weakly bound intermediated in the actomyosin adenosine triphosphatase cycle. *Biophys. J.* 64:454–471

Rayment, I., W. R. Rypniewski, K. Schmidt-Bläse, R. Smith, D. R. Tomchick, M. M. Benning, D. A. Winkelmann, G. Wesenberg, and H. M.

Holden. 1993a. Three-dimensional structure of myosin subfragment-1: a molecular motor. *Science.* 261:50–58.

Rayment, I., H. M. Holden, M. Whittaker, C. B. Yohn, K. C. Holmes, and R. A. Milligan. 1993b. Structure of the actin-myosin complex and its implications for muscle contraction. *Science.* 261:58–65.

Schoenberg, M. 1988. Characterization of the myosin adenosine triphosphate (M-ATP) crossbridge in rabbit and frog skeletal muscle fibers. *Biophys. J.* 54:135–148.

Schröder, R. R., D. J. Manstein, W. Jahn, H. Holden, I. Rayment, K. C. Holmes, and J. A. Spudich. 1993. Three-dimensional atomic model of F-actin decorated with Dictyostelium myosin S1. *Nature.* 364:171–174.

Stein, L. A., R. P. Schwarz, P. B. Chock, and E. Eisenberg. 1979. Mechanism of actomyosin adenosine triphosphatase. Evidence that adenosine 5′-triphosphate hydrolysis can occur without dissociation of the actomyosin complex. *Biochemistry.* 18:3895–3909.

Taylor, E. W. 1991. Kinetic studies of the association and dissociation of myosin subfragment 1 and actin. *J. Biol. Chem.* 266:294–302.

Trybus, K. M., and E. W. Taylor. 1980. Kinetic studies of the cooperative binding of subfragment 1 to regulated actin. *Proc. Natl. Acad. Sci. USA.* 77:7209–7213.

Velaz, L., Y. Chen, J. M. Chalovich. 1993. Characterization of a caldesmon fragment that competes with myosin-ATP binding to actin. *Biophys. J.* 65:892–898.

Wagner, P. D., and E. Giniger. 1981. Calcium-sensitive binding of heavy meromyosin to regulated actin in the presence of ATP. *J. Biol. Chem.* 256:12647–12650.

Walker, M., H. White, B. Belknap, and J. Trinick. 1994. Electron cryomicroscopy of acto-myosin-S1 during steady-state ATP hydrolysis. *Biophys. J.* 66:1563–1572.

White, H. D., and E. W. Taylor. 1976. Energetics and mechanism of actomyosin adenosine triphosphatase. *Biochemsitry.* 15:5818–5826.

Xu, S., B. Brenner, J. M. Chalovich, and L. C. Yu. 1993a. Radial elasticities of attached crossbridges in muscle fibers are state dependent. *Biophys. J.* 64:252*a*. (Abstr.)

Xu, S., B. Brenner, and L. C. Yu. 1993b. State-dependent radial elasticity of attached cross-bridges in single skinned fibers of rabbit psoas muscle. *J. Physiol.* 461:283–299.

Xu, S., S. Malinchik, D. Gilroy, B. Brenner, and L. C. Yu. 1994. Integrated intensities of myosin layer lines are not affected by weak attachment of cross-bridges to actin at 20°C. *Biophys. J.* 66:190*a*. (Abstr.)

Yu, L. C., and B. Brenner. 1989. Structures of actomyosin crossbridges in relaxed and rigor muscle fibers. *Biophys. J.* 55:441–453.